

1 **Title: CRISPR-based kinome-screening revealed MINK1 as a druggable player to rewire**

2 **5FU-resistance in OSCC through AKT/MDM2/p53 axis**

3 **Running title: MINK1 promotes 5FU resistance via AKT/MDM2/p53 axis**

4

5 Sibasish Mohanty^{#1,2}, Pallavi Mohapatra^{#1,2}, Omprakash Shriwas¹, Shamima Azma Ansari^{1,2},

6 Manashi Priyadarshini^{1,3}, Swatismita Priyadarsini¹, Rachna Rath⁴, Mahesh Sultania⁵, Saroj

7 Kumar Das Majumdar⁶, Rajeeb Kumar Swain¹, Rupesh Dash^{1*}

8

9 1. Institute of Life Sciences, Bhubaneswar, Odisha, India-751023

10 2. Regional Center for Biotechnology, Faridabad, India.

11 3. KIIT School of Biotechnology, KIIT University, Bhubaneswar, India.

12 4. Dept. of Oral & Maxillofacial Pathology, SCB Dental College & Hospital, Cuttack, Odisha,

13 India- 753007

14 5. Department of Surgical Oncology, All India Institute of Medical Sciences, Bhubaneswar,

15 Odisha, India-751019

16 6. Department of Radiotherapy, All India Institute of Medical Sciences, Bhubaneswar, Odisha,

17 India-751019

18 [#] Authors contributed equally

19 ^{*} Corresponding authors

20 Rupesh Dash, Institute of Life Sciences, Nalco Square, Chandrasekharpur, Bhubaneswar-

21 751023, Odisha, India. Phone: +91-674-2301460, Fax: +91-674-2300728, E-mail:

22 rupesh.dash@gmail.com , rupeshdash@ils.res.in

23 **The authors declare no potential conflicts of interest.**

24 **Financial support:** Grant support: This work is supported by ICMR (5/13/9/2019-NCD-III),
25 Institute of Life Sciences, Bhubaneswar intramural support and DBT BT/ INF/22/SP28293/2018
26 (for imaging facility).

27 **Keywords: MINK1, 5Fluorouracil, AKT, MDM2, p53, Lestaurtinib, Patient derived cells**

28

29 **Abstract**

30 Cisplatin, 5FU and docetaxel (TPF) are the most common chemotherapy regimen used for
31 advanced OSCC. However, many cancer patients experience relapse, continued tumor growth,
32 and spread due to drug resistance, which leads to treatment failure and metastatic disease. Here,
33 using a CRISPR/Cas9 based kinome knockout screening, Misshapen-like kinase 1 (MINK1) is
34 identified as an important mediator of 5FU resistance in OSCC. Analysis of clinical samples
35 demonstrated significantly higher MINK1 expression in the tumor tissues of chemotherapy non-
36 responder as compared to chemotherapy responders. The nude mice and zebrafish xenograft
37 experiments indicate that knocking out MINK1 restores 5FU mediated cell death in
38 chemoresistant OSCC. An antibody based phosphorylation array screen revealed MINK1 as a
39 negative regulator of p53. Mechanistically, MINK1 modulates AKT phosphorylation at Ser473,
40 which enables p-MDM2 (Ser 166) mediated degradation of p53. We also identified lestaurtinib
41 as a potent inhibitor of MINK1 kinase activity. The patient derived TPF resistant cell based
42 xenograft data suggest that lestaurtinib restores 5FU sensitivity and facilitates a significant
43 reduction of tumor burden. Overall, our study suggests that MINK1 is a major driver of 5FU
44 resistance in OSCC. The novel combination of MINK1 inhibitor lestaurtinib and 5FU needs
45 further clinical investigation in advanced OSCC.

46 **Introduction**

47 Majority of head and neck cancer is originated from mucosal epithelium collectively termed as
48 Oral squamous cell carcinomas (OSCC) ¹. It is the most prevalent neoplasm in developing
49 country like India with approximately 80000 new cases diagnosed every year ². Unfortunately,
50 most of the patients present with advanced OSCC are without having any preclinical history of
51 pre malignant lesions. The treatment modalities for advanced OSCC includes surgical removal of
52 tumor followed by concomitant chemoradiotherapy. Neoadjuvant chemotherapy is frequently
53 prescribed for surgically unresectable OSCC tumors ³. However, despite of having all these
54 treatment modalities the 5-year survival rate of advanced tongue OSCC is less than 50%.
55 Chemoresistance is one of the major causes of treatment failure in OSCC⁴. The
56 chemotherapeutic regimen used for OSCC are cisplatin, 5FU and Docetaxel (TPF)³. Though
57 chemotherapy drugs show initial positive response, tumor acquires resistance gradually and
58 patients experience continued tumor growth and metastatic disease.

59 Reprogramming resistant cells to undergo drug induced cell death is a viable way to overcome
60 drug resistance. This can be achieved by identifying the causative factors for acquired
61 chemoresistance and discovering novel agents to target critical causative factors, which will
62 restore drug-induced cell death in chemoresistant OSCC. Kinases, which transfer a reversible
63 phosphate group to proteins, play important role in regulating several phenotypes of
64 carcinogenesis including growth, proliferation, angiogenesis, metastasis and evasion of antitumor
65 immune responses ⁵. There are approximately 538 known kinases in human which are known to
66 regulate different kinase signaling. A few of them are also known to regulate drug resistance in
67 HNSCC. A kinome study revealed, microtubule-associated serine/threonine kinase 1 (MAST1) is
68 a major driver of cisplatin resistance in HNSCC. MAST1 inhibitor lestaurtinib efficiently

69 sensitized chemoresistant cells to cisplatin. Overall, the study suggests that MAST1 is a viable
70 target to overcome cisplatin resistance ⁶. Ectopic overexpression of receptor tyrosine kinase in
71 HNSCC mediates acquired resistance against cetuximab. For example, hyper activation of AXL
72 was observed in clinical samples those are resistant to cetuximab ⁷. It was also found that RAS-
73 MAPK are key mediator for cetuximab resistance in OSCC ⁸. However, very limited studies are
74 available about the kinases those mediate 5FU resistance in OSCC.

75 MINK1 belongs to germinal center kinase (GCK) family and it is involved in regulation of
76 several important signaling cascades ⁹. Recently, it is reported that MINK1 can regulate the
77 planner cell polarity, which is essential for spreading of cancer cells. The PRICKLE1 encodes
78 the planner cell polarity protein that binds to MINK1 and RICTOR (a member in mTOR2
79 complex) and this complex regulates the AKT mediated cell migration. Selectively targeting
80 either of MINK1, PRICKLE1 or RICTOR can significantly decrease the migration of cancer cell
81 in breast carcinomas ¹⁰. Ste20-related kinase, misshapen (msn), a Drosophila homolog of
82 MINK1 regulates embryonic dorsal closure through activation of c-jun amino-terminal kinase
83 (JNK) ¹¹.

84 The goal of this study is to find out the potential kinase(s) those are major driver(s) of 5FU
85 resistance in OSCC, for which a CRISPR based kinome screening was employed on 5FU
86 resistant OSCC lines. The top ranked protein MINK1 was selected for validation in multiple cell
87 lines and patient derived cells. In addition to this, lestaurtinib was identified to inhibit MINK1
88 kinase activity, which can reverse 5FU mediated cell death in chemoresistant OSCC lines.
89 Ultimately, we demonstrated that MINK1 regulates the p53 in 5FU resistant OSCC. MINK1
90 activates AKT by phosphorylation at Ser473, which phosphorylates MDM2 at Ser166, the later
91 in turn triggers degradation of p53.

92 **Materials and Methods**

93 **Cell culture:** The human tongue OSCC lines (H357, SCC4 and SCC9) were obtained from
94 Sigma Aldrich, sourced from European collection of authenticated cell culture. All OSCC cell
95 lines were cultured and maintained in DMEM F12 supplemented with 10% FBS (Thermo Fisher
96 Scientific), penicillin–streptomycin (Pan Biotech) and 0.5 ug/ml sodium hydrocortisone
97 succinate. HEK 293T cells were maintained in DMEM supplemented with 10% FBS and
98 penicillin–streptomycin (Pan Biotech).

99 **High Content Screening:** 1000 cells/ well were seeded in black flat bottom 96 well plate
100 (Thermo Scientific™ Nunc) and divided into two experimental groups, one without 5FU
101 treatment and the other with 5FU treatment. A CRISPR based kinome-wide screening was
102 performed using a lentiviral sgRNA library (LentiArray™ Human Kinase CRISPR Library,
103 Thermo Fisher Scientific, M3775) that knocks out 840 kinase and kinase related genes
104 individually with total number of 3214 sgRNA constructs. Transduction of lentiviruses (MOI:2)
105 containing pooled sg RNAs (up to 4) targeting each of 840 genes along with positive and
106 negative control lentiviruses into individual wells was carried out in presence of polybrene
107 (8 μ g/ml). At 48 hours post transduction, selection with puromycin (0.5 μ g/ml) was performed for
108 next 2-3 days, followed by treatment of vehicle control and 5FU at sub lethal dose respectively
109 in both groups for 48h. Finally, cells were stained with LIVE/DEAD™ Viability/Cytotoxicity
110 Kit (Thermo Fisher Scientific Cat # L3224) and high content screening was performed using
111 CellInsight CX7 High-Content Screening (HCS) Platform. The green fluorescence indicates the
112 living cells and red fluorescence indicates dead cells. Images from 20 fields per well were
113 acquired using 10X objective lens. Two different fluorescent channels (excitation wavelengths -
114 488nm and 561nm) were used for acquiring images. Image analysis was performed using the

115 HCS Studio software. A threshold value for each channel was set once and used for the entire
116 screening. To identify the cells, segmentation was done. Some of the clumped and poorly
117 segmented cells were excluded from further analysis on the basis of area, shape and intensity. On
118 the basis of intensity, number of live and dead cells were counted and an objective mask (blue
119 lines in the images) was created around each cell. For positive control, Cas9 over expressing
120 cells were transduced with lentiviruses expressing sgRNA targeting human hypoxanthine
121 phosphoribosyltransferase 1 (HPRT1) (LentiArray™ CRISPR Positive Control Lentivirus,
122 human HPRT, Thermo Fisher Scientific Cat # A32829). HPRT1 knockout cells shows resistance
123 to 6-thioguanine (6TG) induced cell death. For negative control, Cas9 over expressing cells were
124 transduced with lentiviruses expressing gRNA with no sequence homology to any region of the
125 human genome (LentiArray™ CRISPR Negative Control Lentivirus, Thermo Fisher Scientific,
126 Cat # A32327).

127 **Patient Derived Xenograft:** BALB/C-nude mice (6-8 weeks, male, NCr-Foxn1nu athymic)
128 were purchased from Hylasco Bio-Technology Pvt. Ltd. For xenograft model early passage of
129 patient-derived cells (PDC2) established from chemo non-responder patient (treated with TPF
130 without having any response) was considered. Two million cells were suspended in phosphate-
131 buffered solution-Matrigel (1:1, 100 μ l) and transplanted into upper flank of mice. The PDC
132 MINK1WT cells were injected in right upper flank and PDC MINK1KO cells were injected in
133 the left upper flank of same mice. These mice were randomly divided into 2 groups (n=5) once
134 the tumors reached a volume of 50 mm^3 and injected with vehicle control or 5FU (10mg/kg)
135 intraperitoneally twice a week. In another experimental set up, PDC2 WT cells were injected in
136 right upper flank of mice. These mice were randomly divided into 4 groups (n=5) after the
137 tumors have reached a volume of 50 mm^3 and injected with vehicle control, 5FU (10mg/kg),

138 Lestaurtinib (20mg/kg) and 5FU (10mg/kg) and Lestaurtinib (20mg/kg) respectively in each
139 individual group, intraperitoneally twice a week. Tumor size was measured using digital Vernier
140 caliper twice a week until the completion of experiments. Tumor volume was determined using
141 the following formula: Tumor volume (mm³) = (minimum diameter)² × (maximum diameter)/2.

142 **Phospho-Protein Profiling:** For performing the Phospho Explorer Antibody Array (Full Moon
143 Biosystems Cat# PEX10), 5X10⁶ number of H3575FUR MINK1WT and H3575FUR
144 MINK1KO cells were seeded and lysates were isolated, after which the protein samples were
145 labelled with biotin as described by manufacturer. Biotinylated protein samples were further
146 blocked in skim milk and were subjected to coupling with the 1318 number of antibodies present
147 on the array slides. Then for the detection of expression of phospho proteins, Cy3-streptavidin
148 (Sigma, Cat#S6402) was added. Array slides were scanned at Fullmoon Biosystems array
149 scanning service and the image analysis was done using ImageJ software.

150 ***In vitro* MINK1 kinase activity assays:** MINK1 Kinase Enzyme System (Promega Cat No#
151 V3911) and ADP-Glo™ Kinase Assay (Promega Cat No#V9101) were procured to perform the
152 *in vitro* kinase assay. Selected compounds (10 μM) were incubated at room temperature for 1 hr
153 with recombinant human MINK1 kinase along with substrate MBP and ATP to perform the
154 kinase reaction using 1X kinase buffer. Further ADP-Glo™ Reagent was added at room
155 temperature for 40 mins to stop the kinase reaction and deplete the unconsumed ATP, hence
156 leaving only ADP. Then Kinase detection reagent was added and incubated at room temperature
157 for 30 mins to convert ADP to ATP and introduce luciferase and luciferin to detect ATP. Finally,
158 the luminescence was measured using VICTOR® Nivo™ Multimode Plate Reader (Perkin
159 Elmer).

160 **Statistical analysis:** All data points are presented as mean and standard deviation and Graph Pad
161 Prism 9.0 was used for calculation. The statistical significance was calculated by one-way
162 variance (one-way ANOVA), Two-Way ANOVA and considered significance at $P \leq 0.05$.

163 **Study approval:** This study was approved by the Institute review Board and Human Ethics
164 committees (HEC) of Institute of Life Sciences, Bhubaneswar (110/HEC/21) and All India
165 Institute of Medical Sciences (AIIMS), Bhubaneswar (T/EMF/Surg.Onco/19/03). The animal
166 related experiments were performed in accordance to the protocol approved by Institutional
167 Animal Ethics Committee of Institute of Life Sciences, Bhubaneswar (ILS/IAEC-204-AH/DEC-
168 20). Approved procedures were followed for patient recruitment and after receiving written
169 informed consent from each patient, tissues samples were collected. Institutional biosafety
170 committee (IBSC) approved all related experiments.

171 **Results**

172 **Establishment and characterization of 5FU resistant OSCC lines:** The 5FU resistant OSCC
173 lines were established by prolonged treatment of 5FU to OSCC cell lines as described in
174 materials and methods. Monitoring the cell viability of 5FU sensitive (5FUS) and resistant
175 (5FUR) pattern of H357, SCC4 and SCC9 cell lines by MTT assay suggest that 5FUR cells
176 achieved acquired resistance (Fig. S1A,B). Enhanced cancer like stem cells (CSCs) and elevated
177 expression of ATP-binding cassette (ABC) transporters are the hallmarks of chemoresistant cells.
178 qRT-PCR data suggest that CSC markers (SOX2, OCT4 and NANOG) as well as majority of
179 ABC transporters expression were elevated in 5FUR cells as compared to 5FUS cells (Fig. S1C,
180 D).

181 **Kinome wide screening identifies MINK1 as a potential driver of 5FU resistance in OSCC:**

182 To identify the kinases those play important role in 5FU resistance, a CRISPR based kinome-
183 wide screening was performed using a lentiviral sgRNA library knocking out 840 kinases
184 individually with a total number of 3214 sgRNA constructs. To target the individual kinase, upto
185 4 sgRNA lentiviral constructs were pooled together. For kinome screening, Cas9 overexpressing
186 5FU resistant OSCC lines were established (Fig. S2), which showed similar drug resistant
187 pattern with parental 5FUR OSCC lines(Fig. S3A). We also determined the polybrenne and
188 puromycin tolerance concentration in Cas9 overexpressing clones (Fig. S3B, C). The 5FUS and
189 5FUR lines were treated with 5FU and cell death was measured in high content analyzer using a
190 fluorescent cell viability dye, the data suggest significantly lower cell death in 5FUR cells as
191 compared to 5FUS cells, which is in harmony with the previously measured 5FU tolerance in
192 both lines (Fig. S4A-C). The screening protocol was optimized using appropriate positive and
193 negative control. When 6TG (6-Thioguanine) was treated to HPRT1 (Hypoxanthine
194 Phosphoribosyltransferase 1) KO lines, which is used as positive control for screening, it showed
195 resistance to cell death, whereas HPRT1 WT cells were sensitive to 6TG, suggesting optimized
196 screening protocol (Fig. S4D, E). As a negative control, lentivirus expressing scrambled sgRNA
197 was used.

198 For primary screening, the 5FU resistant line (H357 5FUR) was transduced with a lentivirus
199 containing sgRNAs targeting each of the 840 individual kinases, after which sub lethal dose of
200 5FU was treated for 48h followed by measuring cell death in high content analyzer using a
201 fluorescent cell viability dye (Fig. 1A). From primary screening, 334 kinases out of 840 were
202 selected for further consideration by rejecting rest of sgRNA clones which alone induced cell
203 death more than 30 % (Fig. 1B, C). The 60 candidate kinases having lowest survival fraction

204 score were evaluated in the secondary screening using three more chemoresistant lines i.e SCC4
205 5FUR, SCC9 5FUR and H357 CisR. From the primary and secondary screening, MINK1, SBK1
206 and FKBP1A emerged as the only three common kinases among the 5FUR lines with MINK1
207 having the lowest survival fraction score, which sensitize the chemoresistant cell to 5FU
208 mediated cell death the most (Fig. 1 C-E). In secondary screening, MINK1 knock out showed
209 minimal efficacy in sensitizing cisplatin resistant cell lines to cisplatin (Fig. 1D), indicating the
210 specific role of MINK1 towards acquired 5FU resistance. Next, monitoring the expression of
211 MINK1 in OSCC resistant lines, we found the expression of MINK1 is significantly higher in
212 5FUR lines as compared to 5FUS lines of OSCC (Fig. 1F). With the evaluation of clinical
213 samples, the expression of MINK1 was found to be elevated in tumor tissues of chemotherapy
214 non-responders as compared to chemotherapy responders (Fig. G, H). We also evaluated the
215 MINK1 expression in drug-naive and post-CT nonresponder paired tumor samples from the
216 same patient and observed that the post-CT-treated tumor samples showed higher MINK1
217 expression (Fig. I, J).

218 **MINK1 is an important target to overcome 5FU resistance in OSCC:** To confirm the
219 finding from the kinome screening, MINK1KO (knock out) clones were generated, using
220 lentivirus expressing two different sgRNAs, in Cas9 overexpressing 5FUR OSCC lines and
221 patient derived line 2 (PDC2) (Fig. S5A). PDC2 was isolated and characterized earlier from
222 tumor of chemotherapy-non-responder patient, who was treated with neoadjuvant TPF without
223 any response ²². The colony forming, MTT and spheroid assay data suggest that knocking out
224 MINK1 significantly reduced the cell viability when the chemoresistant cells were treated with
225 5FU (Fig. S5B, C and Fig.2A). Here onwards we used sgRNA 1 for rest of the experiments.
226 Similarly, knocking out MINK1 induced 5FU mediated cell death in chemoresistant cells (Fig.

227 2B). Enhanced p-H2AX and cleaved PARP was observed in MINK1KO cells followed by
228 treatment with 5FU indicating the potential role of MINK1 in mediating 5FU resistance (Fig.
229 2C,D). Further, to test the in vivo efficacy of the kinome screening data, we implanted PDC2
230 MINK1WT cells into right upper flank and PDC2 MINK1KO cells into the left upper flank of
231 nude mice followed by treatment with 5FU. Treatment with 5FU (10 mg/kg) significantly
232 reduced the tumor burden in the MINK1KO but not in MINK1WT group (Fig. 2E-G).
233 Immunohistochemistry data suggests markedly decreased cell proliferation signal (Ki67) in 5FU-
234 treated MINK1KO tumors (Fig. 2H). Earlier it is known that selective knockdown of MINK1
235 decreases the migration of human breast cancer lines ¹⁰. To evaluate whether depletion of
236 MINK1 also reduces migration of chemoresistant OSCC lines and PDC2, Boyden chamber
237 assays and scratch/wound healing assays were performed. The data suggest that knock out of
238 MINK1 followed by treatment with 5FU significantly reduces the relative number of migrated
239 cells (Fig. S6A). Similarly, scratch area analysis suggest that percentage of scratch area is
240 significantly higher when 5FU is treated to MINK1KO drug resistant cells (Fig. S6B, C). Next,
241 we used Zebrafish (*Danio rerio*) [Tg(fli1:EGFP)] tumor xenograft model to further validate our
242 findings. Equal number of the WT and PDC2MINK1 KO cells were stained with Dil (1,1'-
243 Dioctadecyl-3,3,3',3'-Tetramethylindocarbocyanine Perchlorate) and injected into perivitelline
244 space of 48-hour post fertilized zebrafish embryos. After 3 days of injection, embryos were
245 treated with vehicle control or 5FU (500 μ M). After 5 days of injection, the primary tumors and
246 metastatic distribution of cancer cells were documented using a fluorescence microscope. The
247 tumor growth, as measured by fluorescence intensity of primary tumors, was found to be
248 significantly reduced in the MINK1 KO group with the treatment of 5FU (Fig. 2I, J). Also,

249 cancer cells showed reduced distal migration from the primary site in the case of MINK1 KO
250 5FU treated group (Fig. 2K). These data indicate MINK1 dependency of 5FU resistant OSCC.

251 **Ectopic expression of MINK1 promotes 5FU resistance in OSCC:** To confirm the potential
252 role of MINK1 in 5FU resistance, we performed gain of function study. For this, using a
253 lentiviral approach we generated MINK1ShRNA stable clones in 5FUR lines and PDC2
254 (MINK1UTRKD), where the shRNA targets the 3'UTR of MINK1 mRNA. For ectopic
255 overexpression of MINK1, the MINK1UTRKD cells were transfected with pDESTCMV/TO
256 MINK1 vector (Fig. 3A). The cell viability and cell death data suggest that knocking down
257 MINK1 in 5FUR cells result in sensitizing the resistant cells to 5FU, however ectopic
258 overexpression of MINK1 rescues the 5FU resistant phenotype (Fig. 3B, C). Similarly,
259 immunostaining data suggest enhanced p-H2AX signal in MINK1UTRKD cells, whereas ectopic
260 overexpression of MINK1 reduces the p-H2AX signal indicating rescue of 5FU resistance in
261 OSCC cells (Fig. 3D). We also observed the rescue of cleaved PARP with ectopic expression of
262 MINK1 suggesting reduced cell death (Fig. 3E). Finally, when MINK1 was overexpressed in
263 OSCC sensitive lines, cells showed resistance to 5FU induced cell death (Fig. 3F).

264 **MINK1 downregulates the expression of p53 in chemoresistant OSCC through activation**
265 **of AKT and MDM2:** To understand the specific role of MINK1 in 5FU resistant OSCC, we
266 performed high-throughput phosphorylation profiling with 1,318 site-specific antibodies from
267 over 30 signaling pathways in 5FUR cells stably expressing MINK1KO and MINK1WT. From
268 this study, phosphorylation of p53 at Ser33 and Ser15 were found to be significantly up
269 regulated in MINK1KO cells as compared to MINK1WT cells. In addition to this,
270 phosphorylation of AKT at Ser473 and phosphorylation of MDM2 at Ser166 were found to be
271 down regulated in MINK1KO cells as compared to MINK1WT (Fig. 4A). Further,

272 immunoblotting was performed to validate the finding of phosphorylation profiling antibody
273 array. The data suggest that phosphorylation of p53 at Ser15 and Ser33 is significantly
274 upregulated and phosphorylation of MDM2 at Ser166 is profoundly downregulated in
275 MINK1KO cells as compared to MINK1WT chemoresistant cells (Fig. 4B). OSCC lines H357
276 and SCC4 have mutant p53, whereas MCF7 and HEK 293 have wild type p53 expression.
277 Further, p53 expression was also found to be inversely correlated with MINK1 irrespective of its
278 mutation status. (Fig. 4B, S7). Next, when MINK1 was ectopically overexpressed in MINK1KD
279 (shRNA targeting 3'UTR) clones, downregulation of p53, p-p53 (Ser33) and p-p53 (Ser15) were
280 observed in chemoresistant OSCC lines (Fig. 4C). In harmony to our finding of phosphorylation
281 array, p-AKT(Ser473) was found to be down regulated in MINK1 depleted cells, which was
282 rescued with ectopic overexpression of MINK1 (Fig. 4 D, E). To confirm the potential role of
283 AKT in modulating MINK1 mediated p53 regulation, we ectopically overexpressed
284 constitutively active AKT (myrAKT) in MINK1KO cells. The immunoblotting data suggest that
285 expression of p53, p-p53 (Ser33) and p-p53 (Ser15) were downregulated when MyrAKT was
286 overexpressed in MINK1KO cells (Fig. 4F). Similarly, when MINK1 over expressing cells were
287 treated with AKT inhibitor (Akti-1/2) , the p53 expression was rescued along with
288 downregulation of p-MDM2 (Ser166) (Fig. 4G). p53 target genes were also evaluated in MINK1
289 KO cells and the immunoblotting data suggest that expression of p21, NOXA and TIGAR in
290 MINK1KO clones were upregulated as compared to MINK1WT clones (Fig. 4H).

291 **Evaluation of Lestaurtinib as MINK1 inhibitor to reverse 5FU resistance in OSCC:** From
292 the screening data, we observed that MINK1 expression is elevated in chemoresistant OSCC and
293 genetic inhibition of the same sensitizes drug resistant lines to 5FU induced cell death. Hence,
294 MINK1 can be a potential therapeutic target to overcome chemoresistance in OSCC. Very

295 limited information on the inhibitors of MINK1 is available in the literature. Hence, we looked
296 for the potential MINK1 inhibitors in the international union of basic and clinical pharmacology
297 (IUPHAR) database, where a screen of 72 inhibitors against 456 human kinases binding activity
298 is provided. Among the potential twelve MINK1 inhibitors, we tested the MINK1 inhibitory
299 activity of three inhibitors i.e., staurosporine, pexmetinib and lestaurtinib. The kinase assay data
300 suggest that lestaurtinib and pexmetinib have highest inhibitory activity for MINK1 (Fig. 5A).
301 The 50% MINK1 inhibitory activity was observed at concentration of 100 nM in case of
302 lestaurtinib and 10 μ M for pexmetinib (Fig. 5B). Next, cell viability assay was performed to
303 select a dose of lestaurtinib and pexmetinib that does not affect cell viability when treated alone
304 (viability > 80%) in 5FU resistant OSCC lines (Fig. 5C, D). Further, the cell viability, spheroid
305 assay and cell death data suggest that the selected sub lethal dose of lestaurtinib (50nM) and
306 pexmetinib (500 μ M) can efficiently restore 5FU mediated cell death in chemoresistant OSCC
307 lines and PDC2 (Fig. 5 E, F and S8A). The IC50 value of 5FU in H3575FUR is 20.49 μ M,
308 however combination of lestaurtinib (50nM) decreases the IC50 value to 4.82 μ M and
309 combination of pexmetinib (500 μ M) lowers the IC50 value of 5FU to 7.08 μ M (Fig. 5 E). As
310 lestaurtinib, with a much lower concentration (50nM) as compared to pexmetinib (500nM)
311 sensitize 5FU to chemoresistant cells, from here on lestaurtinib was considered for rest of the
312 study. Enhanced expression of p-H2AX and cleaved PARP was observed only in combination
313 group with lestaurtinib and 5FU indicating programmed cell death (Fig. 5G and S8B). Boyden
314 chamber assays data suggests that combinatorial treatment of lestaurtinib and 5FU
315 significantly reduces the relative number of migrated cells (Fig S8C). In harmony to the
316 observation made by knockout of MINK1 in chemoresistant cells, we also found that lestaurtinib
317 significantly decreased the phosphorylation of MDM2(Ser166) and AKT(Ser473) and elevated

318 the expression of p53 in chemoresistant cells (Fig. 5H). Further, we found that lestaurtinib failed
319 to sensitize 5FU mediated cell death in MINK1 knocked out 5FUR lines (Fig. 5I), which
320 suggests that lestaurtinib conferred 5FU sensitivity by inhibiting MINK1 kinase activity. To
321 check the in vivo efficacy of this novel combination, nude mice xenograft model was performed
322 using patient derived cells (PDC2). The in vivo data suggest that the combination of lestaurtinib
323 (20mg/kg) and 5FU (10mg/kg) profoundly reduced the tumor burden as compared to treatment
324 with either of the single agents (Fig. 6A-C). Immunohistochemistry data suggest significant
325 reduction in CD44 and Ki67 expression along with increased expression of cleaved caspase 3 in
326 combination group (Fig. 6D). Finally, we performed combinatorial anti-tumor effect of non-
327 cytotoxic extremely low dose of cisplatin (1 μ M), 5FU (1 μ M) and lestaurtinib (50nM) in PDC2.
328 The cell viability, cell death, western blotting and colony forming assay data suggest
329 significantly higher cell death in cisplatin, 5FU and lestaurtinib combinatorial group, as
330 compared to any other possible combinatorial group, i.e. 5FU and lestaurtinib or cisplatin and
331 lestaurtinib or cisplatin and 5FU (Fig. S8).

332 **Discussion:** The hallmark chemoresistant phenotypes of cancer cells are reduced apoptosis,
333 altered metabolic activity, enhanced cancer stem cells like population, increased drug efflux and
334 decreased drug accumulations. However, the causative factors which are responsible for acquired
335 chemoresistance is largely not known. It is well known that kinases play key role in various
336 processes of carcinogenesis and kinase inhibitors are established as potential anti-tumor agents.
337 In this study, for the first time, we have performed a kinome screening in drug resistant cancer
338 cells to explore the potential kinase(s) those mediate 5FU resistance in OSCC. From the primary
339 and secondary kinome screening, MINK1 was found to be top ranked kinase that can re-sensitize
340 drug resistant cells to 5FU. Overall, MINK1 is known to regulate cell senescence, cell motility

341 and migration. Till date the potential role of MINK1 in modulating chemoresistance is still
342 unknown. Here in this study, we found the novel function of MINK1 by which it regulates 5FU
343 resistance in OSCC.

344 To understand the mechanism by which MINK1 regulates 5FU resistance, we performed a high-
345 throughput phosphorylation profiling in 5FUR cells stably expressing MINK1sgRNA. From this
346 study, we found p- p53 (Ser33) and p-53(Ser15) to be significantly up-regulated in MINK1KO
347 cells and p-AKT (Ser473) and p-MDM2 (Ser166) were found to be down-regulated in
348 MINK1KO cells as compared to MINK1WT. The tumor suppressor p53 is phosphorylated at
349 various amino acids by different kinases, which tightly regulates its stability ²³. It is well known
350 that MDM2 (a E3 ubiquitin ligase) acts as a negative regulator of p53. MDM2 forms a complex
351 with p53 and facilitates the recruitment of ubiquitin molecules for its degradation ²⁴. Earlier, it
352 was established that insulin induced activated AKT (Ser473) phosphorylates MDM2 at Ser 166
353 and Ser 186, which can lead to MDM2 mediated proteasomal degradation of p53 in cytoplasm
354 as well as in nucleus ^{25, 26}. These events lead to blocking of p53-mediated transcription of genes
355 those generally involve in apoptosis, cell cycle regulation and senescence. In addition to this,
356 p53 is phosphorylated at Ser15 by ATM, DNA-PK and ATR in response to DNA damage ^{27, 28},
357 ²⁹. Hence, phosphorylation of Ser15 and Ser33 leads to activation and stabilization of p53 as they
358 attenuate the MDM2 mediated degradation of p53 ^{30, 31}. Overall, in this study we found that
359 MINK1 regulates the expression of p53 through activation of AKT which in turns triggers p-
360 MDM2 (Ser 166) (Figure 6 E).

361 Jin et al 2018 performed a kinome screening in cisplatin resistant cells to explore the potential
362 kinases those confer cisplatin resistance in HNSCC. The data suggests that microtubule-
363 associated serine/threonine-protein kinase 1 (MAST1) mediates cisplatin resistance in HNSCC

364 by phosphorylating MEK1, triggering cRaf-independent activation of MEK1, which led to down
365 regulation of BH3 only protein BIM. Jin et al 2018 also found that lestaurtinib to be a potent
366 inhibitor of MAST1. Lestaurtinib successfully restores the cisplatin induced cell death in
367 cisplatin resistant cells ⁶. Lestaurtinib not only inhibits MAST1 activity but also known as an
368 inhibitor of JAK2, Trk and FLT3 ^{32,33}. In this study, we found that lestaurtinib inhibits activity of
369 MINK1 and lestaurtinib can resensitize the drug resistant OSCC to 5FU. The most common
370 chemotherapy regimen for OSCC is the combination of cisplatin, 5FU and Docetaxel (TPF).
371 Finally, our data suggests that combination of extremely low dose of cisplatin (1 μ M), 5FU
372 (1 μ M) and lestaurtinib (50nM) can overcome chemoresistance in OSCC (Fig. S8). Currently
373 lestaurtinib alone or in combination with other chemotherapy drug is under clinical investigation
374 (phase II) for patients having AML and it is well tolerated in human beings ³⁴.

375 Overall, our data suggests that MINK1 is a mediator of 5FU resistance in OSCC. Besides this,
376 though we have demonstrated that MINK1 negatively regulates P53 through AKT/MDM2 axis
377 in 5FU resistant OSCC, the 5FU specificity of this MINK1 driven signalling cascade remains to
378 be fully elucidated. Further, genetic or pharmacological (Lestaurtinib) inhibition of MINK1
379 successfully resensitized chemo resistant lines to 5FU. This novel combination of 5FU and
380 Lestaurtinib needs further clinical investigation.

381 **Acknowledgements:** PM is a CSIR-SRF, SM is UGC-SRF, SAA is a UGC-JRF.

382 **Author contribution:** SM, PM, OS, MP, SAA and SP performed experiments, and analyzed the
383 data, under the direction of R.D. RR, MS and S.K.M. performed part of experiments. SM, PM,
384 RKS and R.D. designed experiments and supervised the study. R.D wrote the manuscript. All
385 authors approved the final version.

386 **Competing interests:** The authors declare no conflict of interest.

387

388

389 **References**

390 1. Johnson DE, Burtness B, Leemans CR, Lui VWY, Bauman JE, Grandis JR. Head and
391 neck squamous cell carcinoma. *Nat Rev Dis Primers* 2020, **6**(1): 92.

392

393 2. Chaturvedi A, Husain N, Misra S, Kumar V, Gupta S, Akhtar N, *et al.* Validation of the
394 Brandwein Gensler Risk Model in Patients of Oral Cavity Squamous Cell Carcinoma in
395 North India. *Head Neck Pathol* 2020, **14**(3): 616-622.

396

397 3. Vishak S, Rangarajan B, Kekatpure VD. Neoadjuvant chemotherapy in oral cancers:
398 Selecting the right patients. *Indian journal of medical and paediatric oncology : official
399 journal of Indian Society of Medical & Paediatric Oncology* 2015, **36**(3): 148-153.

400

401 4. Maji S, Panda S, Samal SK, Shriwas O, Rath R, Pellecchia M, *et al.* Bcl-2 Antiapoptotic
402 Family Proteins and Chemoresistance in Cancer. *Advances in cancer research* 2018, **137**:
403 37-75.

404

405 5. Gross S, Rahal R, Stransky N, Lengauer C, Hoeflich KP. Targeting cancer with kinase
406 inhibitors. *J Clin Invest* 2015, **125**(5): 1780-1789.

407

408 6. Jin L, Chun J, Pan C, Li D, Lin R, Alesi GN, *et al.* MAST1 Drives Cisplatin Resistance
409 in Human Cancers by Rewiring cRaf-Independent MEK Activation. *Cancer cell* 2018,
410 **34**(2): 315-330 e317.

411

412 7. Brand TM, Iida M, Stein AP, Corrigan KL, Braverman CM, Luthar N, *et al.* AXL
413 mediates resistance to cetuximab therapy. *Cancer research* 2014, **74**(18): 5152-5164.

414

415 8. Rampias T, Giagini A, Siolos S, Matsuzaki H, Sasaki C, Scorilas A, *et al.* RAS/PI3K
416 crosstalk and cetuximab resistance in head and neck squamous cell carcinoma. *Clin
417 Cancer Res* 2014, **20**(11): 2933-2946.

418

419 9. Dan I, Watanabe NM, Kobayashi T, Yamashita-Suzuki K, Fukagaya Y, Kajikawa E, *et
420 al.* Molecular cloning of MINK, a novel member of mammalian GCK family kinases,
421 which is up-regulated during postnatal mouse cerebral development. *FEBS Lett* 2000,
422 **469**(1): 19-23.

423

424 10. Daulat AM, Bertucci F, Audebert S, Serge A, Finetti P, Josselin E, *et al.* PRICKLE1
425 contributes to Cancer Cell Dissemination through Its Interaction with mTORC2.
426 *Developmental cell* 2016, **37**(4): 311-325.

427

428 11. Su YC, Treisman JE, Skolnik EY. The Drosophila Ste20-related kinase misshapen is
429 required for embryonic dorsal closure and acts through a JNK MAPK module on an
430 evolutionarily conserved signaling pathway. *Genes Dev* 1998, **12**(15): 2371-2380.

431

432 12. Sanjana NE, Shalem O, Zhang F. Improved vectors and genome-wide libraries for
433 CRISPR screening. *Nat Methods* 2014, **11**(8): 783-784.

434

435 13. Tzelepis K, Koike-Yusa H, De Braekeleer E, Li Y, Metzakopian E, Dovey OM, *et al.* A
436 CRISPR Dropout Screen Identifies Genetic Vulnerabilities and Therapeutic Targets in
437 Acute Myeloid Leukemia. *Cell Rep* 2016, **17**(4): 1193-1205.

438

439 14. Shriwas O, Arya R, Mohanty S, Mohapatra P, Kumar S, Rath R, *et al.* RRB1P1 rewrites
440 cisplatin resistance in oral squamous cell carcinoma by regulating Hippo pathway. *Br J
441 Cancer* 2021, **124**(12): 2004-2016.

442

443 15. Moffat J, Grueneberg DA, Yang X, Kim SY, Kloepfer AM, Hinkle G, *et al.* A lentiviral
444 RNAi library for human and mouse genes applied to an arrayed viral high-content screen.
445 *Cell* 2006, **124**(6): 1283-1298.

446

447 16. Samal SK, Routray S, Veeramachaneni GK, Dash R, Botlagunta M. Ketorolac salt is a
448 newly discovered DDX3 inhibitor to treat oral cancer. *Scientific reports* 2015, **5**: 9982.

449

450 17. Shriwas O, Priyadarshini M, Samal SK, Rath R, Panda S, Das Majumdar SK, *et al.*
451 DDX3 modulates cisplatin resistance in OSCC through ALKBH5-mediated m(6)A-
452 demethylation of FOXM1 and NANOG. *Apoptosis* 2020, **25**(3-4): 233-246.

453

454 18. Mohapatra P, Shriwas O, Mohanty S, Ghosh A, Smita S, Kaushik SR, *et al.* CMTM6
455 drives cisplatin resistance by regulating Wnt signaling through the ENO-
456 1/AKT/GSK3beta axis. *JCI Insight* 2021, **6**(4).

457

458 19. Johannessen CM, Boehm JS, Kim SY, Thomas SR, Wardwell L, Johnson LA, *et al.* COT
459 drives resistance to RAF inhibition through MAP kinase pathway reactivation. *Nature*
460 2010, **468**(7326): 968-972.

461

462 20. Campeau E, Ruhl VE, Rodier F, Smith CL, Rahmberg BL, Fuss JO, *et al.* A versatile
463 viral system for expression and depletion of proteins in mammalian cells. *PloS one* 2009,
464 **4**(8): e6529.

465

466 21. Ramaswamy S, Nakamura N, Vazquez F, Batt DB, Perera S, Roberts TM, *et al.*
467 Regulation of G1 progression by the PTEN tumor suppressor protein is linked to
468 inhibition of the phosphatidylinositol 3-kinase/Akt pathway. *Proc Natl Acad Sci U S A*
469 1999, **96**(5): 2110-2115.

470

471 22. Maji S, Shriwas O, Samal SK, Priyadarshini M, Rath R, Panda S, *et al.* STAT3- and
472 GSK3beta-mediated Mcl-1 regulation modulates TPF resistance in oral squamous cell
473 carcinoma. *Carcinogenesis* 2019, **40**(1): 173-183.

474

475 23. Maclaine NJ, Hupp TR. The regulation of p53 by phosphorylation: a model for how
476 distinct signals integrate into the p53 pathway. *Aging (Albany NY)* 2009, **1**(5): 490-502.

477

478 24. Moll UM, Petrenko O. The MDM2-p53 interaction. *Mol Cancer Res* 2003, **1**(14): 1001-
479 1008.

480

481 25. Gottlieb TM, Leal JF, Seger R, Taya Y, Oren M. Cross-talk between Akt, p53 and
482 Mdm2: possible implications for the regulation of apoptosis. *Oncogene* 2002, **21**(8):
483 1299-1303.

484

485 26. Mayo LD, Donner DB. A phosphatidylinositol 3-kinase/Akt pathway promotes
486 translocation of Mdm2 from the cytoplasm to the nucleus. *Proc Natl Acad Sci U S A*
487 2001, **98**(20): 11598-11603.

488

489 27. Khanna KK, Keating KE, Kozlov S, Scott S, Gatei M, Hobson K, *et al.* ATM associates
490 with and phosphorylates p53: mapping the region of interaction. *Nat Genet* 1998, **20**(4):
491 398-400.

492

493 28. Lakin ND, Hann BC, Jackson SP. The ataxia-telangiectasia related protein ATR mediates
494 DNA-dependent phosphorylation of p53. *Oncogene* 1999, **18**(27): 3989-3995.

495

496 29. Shieh SY, Ikeda M, Taya Y, Prives C. DNA damage-induced phosphorylation of p53
497 alleviates inhibition by MDM2. *Cell* 1997, **91**(3): 325-334.

498

499 30. Sakaguchi K, Herrera JE, Saito S, Miki T, Bustin M, Vassilev A, *et al.* DNA damage
500 activates p53 through a phosphorylation-acetylation cascade. *Genes Dev* 1998, **12**(18):
501 2831-2841.

502

503 31. Yagosawa S, Yoshida K. Tumor suppressive role for kinases phosphorylating p53 in
504 DNA damage-induced apoptosis. *Cancer Sci* 2018, **109**(11): 3376-3382.

505

506 32. Hexner EO, Serdikoff C, Jan M, Swider CR, Robinson C, Yang S, *et al.* Lestaurtinib
507 (CEP701) is a JAK2 inhibitor that suppresses JAK2/STAT5 signaling and the
508 proliferation of primary erythroid cells from patients with myeloproliferative disorders.
509 *Blood* 2008, **111**(12): 5663-5671.

510

511 33. Shabbir M, Stuart R. Lestaurtinib, a multitargeted tyrosine kinase inhibitor: from bench
512 to bedside. *Expert Opin Investig Drugs* 2010, **19**(3): 427-436.

513

514 34. Knapper S, Burnett AK, Littlewood T, Kell WJ, Agrawal S, Chopra R, *et al.* A phase 2
515 trial of the FLT3 inhibitor lestaurtinib (CEP701) as first-line treatment for older patients
516 with acute myeloid leukemia not considered fit for intensive chemotherapy. *Blood* 2006,
517 **108**(10): 3262-3270.

518 **Figure Legends**

519 **Figure 1: CRISPR based Kinome screening revealed MINK1 as a potential mediator for**
520 **5FU resistance in OSCC. A)** Schematic presentation of approach for CRSPR/Cas9 based
521 kinome knockout screening to discover the potential kinase responsible for 5FU resistance in
522 OSCC. **B-C)** Primary screening of 840 kinases was performed with sublethal dose of 5FU
523 (8 μ M). The kinases (n=506 nos) whose knockout alone induced significantly higher cell death (>
524 30%) depicted in red were excluded. From the rest of the kinases (n=334 nos) depicted in green,
525 the survival fraction (5FU treated/ Vehicle Control) was determined and top 60 candidates
526 having lowest survival fraction were considered for secondary screening. **D)** For secondary
527 screening with top 60 kinases, four cell lines were considered i.e., H357 5FUR, SCC4 5FUR,
528 SCC9 5FUR and H357CisR. After overlapping all three 5FUR cell lines, MINK1, SBK1,
529 FKB1A were found to be the common kinases among them. MINK1 was selected as a potential
530 kinase target purely based on having the lowest survival fraction among all common candidates.
531 **E)** The fluorescent images acquired from high content analyzer with indicated treated group
532 during kinome screening. **F)** Lysates were collected from indicated cells and immunoblotting
533 was performed with indicated antibodies. **G)** Protein expression of MINK1 was analyzed by IHC
534 in chemotherapy- responder and chemotherapy-non-responder OSCC tumors. Scale bars: 50 μ m.
535 **H)** IHC scoring for MINK1 from panel G (Q Score =Staining Intensity \times % of Staining),
536 (Median, n=11 for chemotherapy-responder and n=23 for chemotherapy-non-responder) *P <

537 0.05 by 2-tailed Student's t test. **I**) Protein expression of MINK1 was analyzed by
538 immunohistochemistry (IHC) in pre- and post-TPF treated paired tumor samples from
539 chemotherapy-non-responder patients. Scale bars: 50 μ m. **J**) IHC scoring for MINK1 from panel
540 I (Q Score =Staining Intensity \times % of IHC Staining). * $P < 0.05$ by 2-tailed Student's t test.

541 **Figure 2: Selectively targeting MINK1 restores 5FU induced cell death in chemoresistant**
542 **OSCC: A)** 5FU resistant cells stably expressing MINK1sgRNA (#1 and #2) and NTsgRNA
543 were treated with 5FU for 48h and cell viability was determined by MTT assay (n=3 and 2-way
544 ANOVA). **B)** Indicated cells were treated with 5FU for 48h, after which cell death was
545 determined by annexin V/7AAD assay using flow cytometer. Bar diagrams indicate the
546 percentage of cell death (early and late apoptotic) with respective treated groups (Mean \pm SEM,
547 n=3, Two-way ANOVA). **C)** Indicated cells were treated with 5 μ M of 5FU for 48h, after which
548 immunostaining was performed for γ -H2AX. **D)** Indicated cells were treated with 5FU for 48h
549 and immunoblotting was performed with indicated antibodies. **E)** PDC2 MINK1WT cells were
550 implanted in right upper flank of athymic male nude mice and PDC2 MINK1KO cells were
551 implanted in left upper flank, after which they were treated with 5FU at indicated concentration.
552 At the end of the experiment mice were euthanized, tumors were isolated and photographed
553 (n=5). **F)** Tumor growth was measured in indicated time points using digital slide caliper and
554 plotted as a graph (mean \pm SEM, n = 5). Two-way ANOVA. **G)** Bar diagram indicates the tumor
555 weight measured at the end of the experiment (mean \pm SEM, n = 5). Two-way ANOVA. **H)**
556 After completion of treatment, tumors were isolated and paraffin-embedded sections were
557 prepared as described in materials and methods to perform immunohistochemistry with indicated
558 antibodies. Scale bars: 50 μ m. **I, J)** Lateral view of fluorescent transgenic [Tg(fli1:EGFP)]
559 zebrafish embryos at Day 0 and Day 5 injected with Dil-Red stained PDC2 control and MINK1

560 KO cells with and without treatment of 5FU (**J**). The tumor growth and migration was assessed
561 by an increase in fluorescence intensity on the 5th day compared to the day of injection. n=6.
562 The quantitation of fluorescence intensity (**I**) was performed using ImageJ software and
563 represented as fold change of fluorescence intensity where day 0 reading was taken as baseline.
564 **K)** Zoomed image of distal part of embryo (5days post injection) to monitor migration of tumor
565 cells.

566 **Figure 3: Ectopic overexpression of MINK1 rescued the drug resistant phenotype in**
567 **MINK1KD drug resistant OSCC: A)** Using a lentiviral approach, 5FU resistant OSCC lines
568 and PDC2 were stably transfected with ShRNA which targets 3'UTR of MINK1 mRNA
569 (MINK1 UTRKD). For ectopic overexpression, pLenti CMV/TO Puro DEST MINK1 and
570 control vector were transiently transfected to indicated MINK1 UTRKD cells and
571 immunoblotting (n=3) was performed with indicated antibodies. **B)** MINK1 was ectopically
572 overexpressed in 5FUR cells stably expressing MINK1ShRNA targeting UTR and treated with
573 5FU at indicated concentration for 48 h, after which cell viability was determined by MTT assay
574 (n=3), 2-way ANOVA. **C)** Cells were treated as indicated in B panel and cell death (early and
575 late apoptotic) was determined by annexin V/7AAD assay using flow cytometer. Bar diagrams
576 indicate the percentage of cell death with respective treated groups (Mean \pm SEM, n=3), 2-way
577 ANOVA. **D)** MINK1 was overexpressed in 5FUR cells stably expressing MINK1ShRNA
578 targeting UTR and treated with 5FU for 48h, after which immunostaining was performed for γ -
579 H2AX as described in materials and methods. **E)** MINK1 was overexpressed in chemoresistant
580 cells stably expressing MINK1ShRNA targeting 3' UTR, followed by 5FU treatment for 48
581 hours, and immunoblotting (n = 3) was performed with indicated antibodies. **F)** 5FU sensitive
582 OSCC lines were transfected with pLenti CMV/TO Puro DEST MINK1 followed by treatment

583 with 5FU at indicated concentration for 48h, after which cell viability was determined by MTT
584 assay (n=3), 2-way ANOVA.

585 **Figure 4: MINK1 regulates the expression of p53 in 5FU resistant OSCC lines through**
586 **AKT/MDM2**

587 **A)** High-throughput phosphorylation profiling with 1,318 site-specific antibodies from over 30
588 signaling pathways was performed in the lysates of MINK1KO and MINK1WT clones of H357
589 5FUR cells as described in methods. The top 20 upregulated phosphoproteins (MINK1
590 KO/MINK1WT) is represented in left panel, whereas top 20 downregulated phosphorylated
591 proteins is represented in right panel. The upregulated targets considered in the study is marked
592 in green red box, whereas downregulated targets in green box. **B)** Lysates were collected from
593 indicated cells and immunoblotting was performed with indicated antibodies. **C)**
594 pDESTCMV/TO MINK1 (ectopic overexpression of MINK1) was transiently transfected in
595 5FUR lines stably expressing MINK1 ShRNA (targeting 3'UTR) and immunoblotting was
596 performed with indicated antibodies. **D)** Lysates were collected from indicated cells and
597 immunoblotting was performed with indicated antibodies. **E)** MINK1 was ectopically
598 overexpressed in 5FUR lines stably expressing MINK1 ShRNA (targeting 3'UTR) and
599 immunoblotting was performed with indicated antibodies. **F)** pLNCX myr HA Akt1 (ectopic
600 overexpression of myr AKT) was transiently transfected in indicated MINK1KO cells and
601 immunoblotting was performed with indicated antibodies. **G)** MINK1 was ectopically
602 overexpressed in 5FUR lines stably expressing MINK1ShRNA (UTRKD) as described in panel
603 C and treated with AKT inhibitor (Akti-1/2) for 24h and immunoblotting was performed with
604 indicated antibodies. **H)** Lysates were collected from indicated cells and immunoblotting was
605 performed with indicated antibodies.

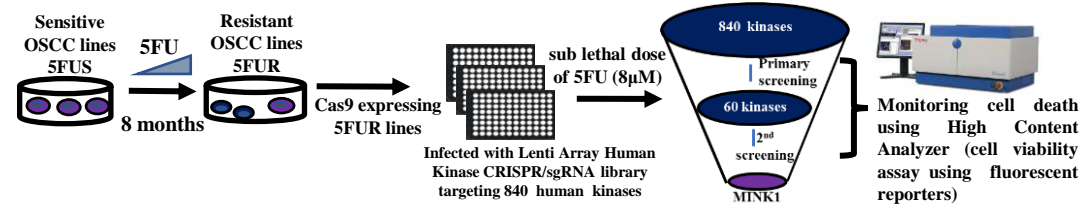
606 **Figure 5: Evaluation of Lestaurtinib as a MINK1 inhibitor to restore 5FU sensitivity in**
607 **drug resistant OSCC: A)** *In vitro* MINK1 kinase assay was performed using three compounds
608 potentially binding to MINK1 (based on IUPHAR database). All compounds (10 μ M) were
609 incubated with recombinant human MINK1 along with substrate MBP and ATP and further
610 subjected to ADP-Glo™ Kinase Assay as described in materials and methods section. **B)**
611 Determination of EC50 value for kinase activity of top two MINK1 inhibitors selected from
612 panel (A). **C-D)** Selection of highest dose of Lestaurtinib and Pexmetinib that does not affect cell
613 viability when treated alone (viability > 80%) in 5FU resistant OSCC lines (n=3), 2-way
614 ANOVA. **E)** 5FU resistant cells were treated with indicated dose of MINK1 inhibitor (50 nM
615 Lestaurtinib, 500 nM Pexmetinb) in combination with increasing concentrations of 5FU for 48
616 h, after which cell viability was determined by MTT assay (n=3), 2-way ANOVA. **F)** 5FU
617 resistant OSCC lines and PDC2 cells were treated indicated dose of MINK1 inhibitor (50 nM
618 Lestaurtinib, 500 nM Pexmetinb) in combination with increasing concentrations of 5FU for 48
619 h, after which cell death (early and late apoptotic) was determined by annexin V/7AAD assay
620 using flow cytometer. Bar diagrams indicate the percentage of cell death with respective treated
621 groups (Mean \pm SEM, n=3). Two-way ANOVA. **G)** Indicated 5FU resistant OSCC lines and
622 PDC2 cells were treated with 5 μ M of 5FU and/or 50nM of Lestaurtinib for 48h, after which
623 immunostaining was performed for γ -H2AX as described in materials ad methods. **H)** Indicated
624 5FU resistant OSCC lines and PDC2 cells were treated with Lestaurtinib for 48h, after which
625 immunoblotting was performed with indicated antibodies. **I)** Effect on 5FU IC50 upon
626 Lestaurtinib treatment in cells with or without MINK1 knockout in indicated 5FU resistant
627 OSCC lines and PDC2 cells (n=3), *P < 0.05 by 2-way ANOVA.

628 **Figure 6: Lestaurtinib and 5FU synergistically reduced tumor burden *in vivo* in drug**
629 **resistant OSCC: A)** Patient-derived cells (PDC2) were earlier established from tumor of
630 chemotherapy (TPF) non-responder patient. PDC2 were implanted in the right upper flank of
631 athymic male nude mice, after which they were treated with 5FU and/or Lestaurtinib at indicated
632 concentrations. At the end of the experiment mice were euthanized, and tumors were isolated and
633 photographed (n = 5). **B)** Bar diagram indicates the tumor weight measured at the end of the
634 experiment (mean \pm SEM, n = 5). Two-way ANOVA. **C)** Tumor growth was measured at the
635 indicated time points using digital slide caliper and plotted as a graph (mean \pm SEM, n = 5).
636 Two-way ANOVA. **D)** After completion of treatment, tumors were isolated, and paraffin-
637 embedded sections were prepared as described in Methods to perform IHC with indicated
638 antibodies. Scale bars: 50 μ m. **E)** Schematic presentation of the mechanism by which MINK1
639 regulates p53 expression through AKT/MDM2 axis.

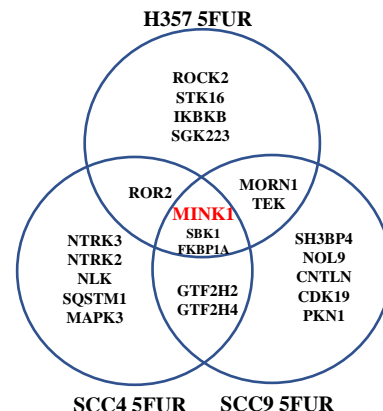
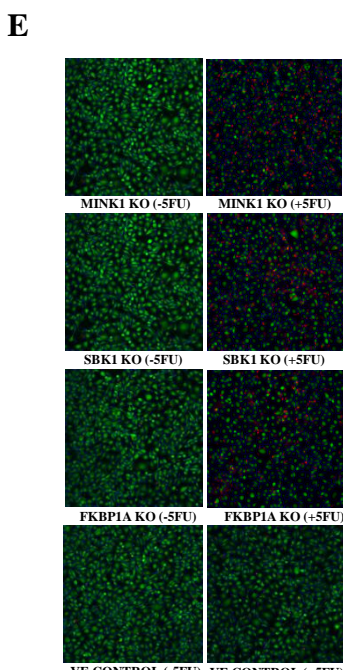
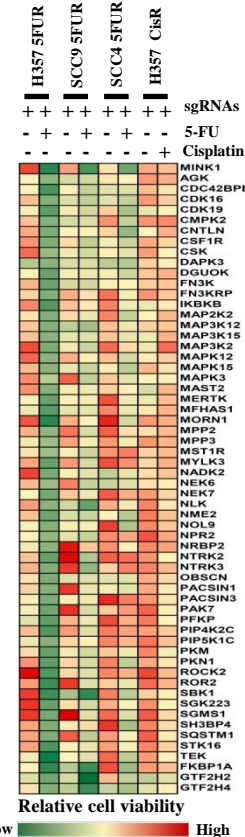
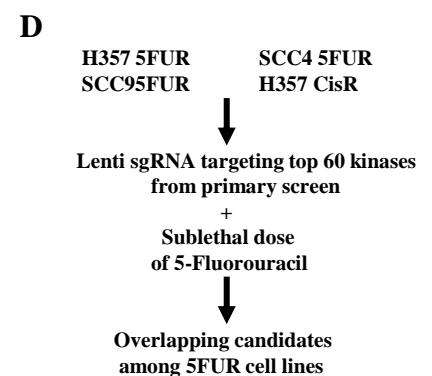
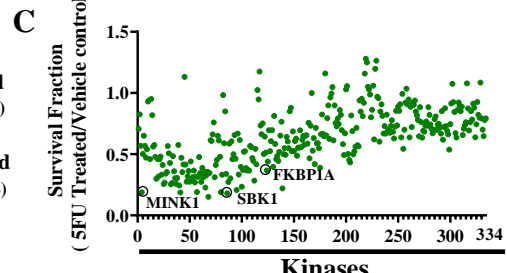
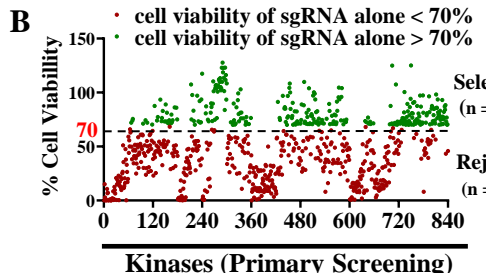
640 **Figure 7: Evaluation of combinatorial anti-tumor effect of low dose of cisplatin, 5FU and**
641 **lestaurtinib in TPF resistant patient derived cells (PDC2). A-B)** PDC2 cells were treated with
642 indicated concentrations of cisplatin, 5FU and lestaurtinib for 48h and cell viability was
643 measured by MTT assay(n=3 and *P < 0.05 by 2-way ANOVA). **C)** PDC2 cells were treated
644 with indicated concentrations of cisplatin, 5FU and lestaurtinib for 48h after which cell death
645 was determined by annexin V/7AAD assay using flow cytometer. Bar diagrams indicate the
646 percentage of cell death (early and late apoptotic) with respective treated groups (Mean \pm SEM,
647 n=3 by Two-way ANOVA). **D)** PDC2 cells were treated with indicated concentrations of
648 cisplatin, 5FU and lestaurtinib for 48h and immunoblotting was performed with indicated
649 antibodies. **E)** PDC2 cells were treated with indicated concentrations of cisplatin, 5FU,
650 lestaurtinib for 12 days and colony forming assays were performed as described in method

651 section. Left panel: Bar diagram indicate the relative colony number (n=3 and *P < 0.05 by 2-
652 way ANOVA). Right panel: representative photographs of colony forming assay in each group.

Figure 01



Strategy for CRISPR based kinome knock out screening in 5FU resistant OSCC lines



Secondary kinase screening in 5FU-resistant OSCC

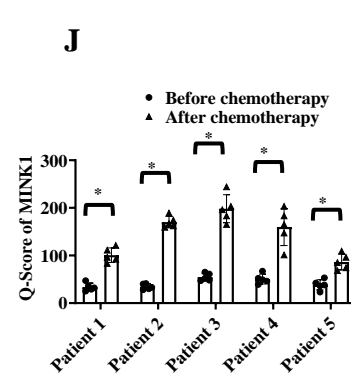
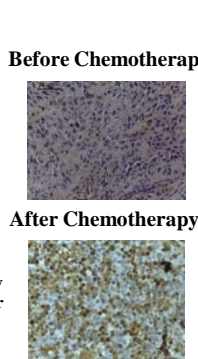
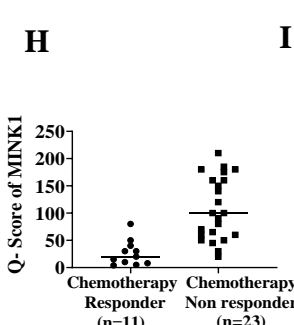
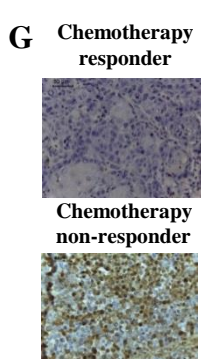


Figure 02

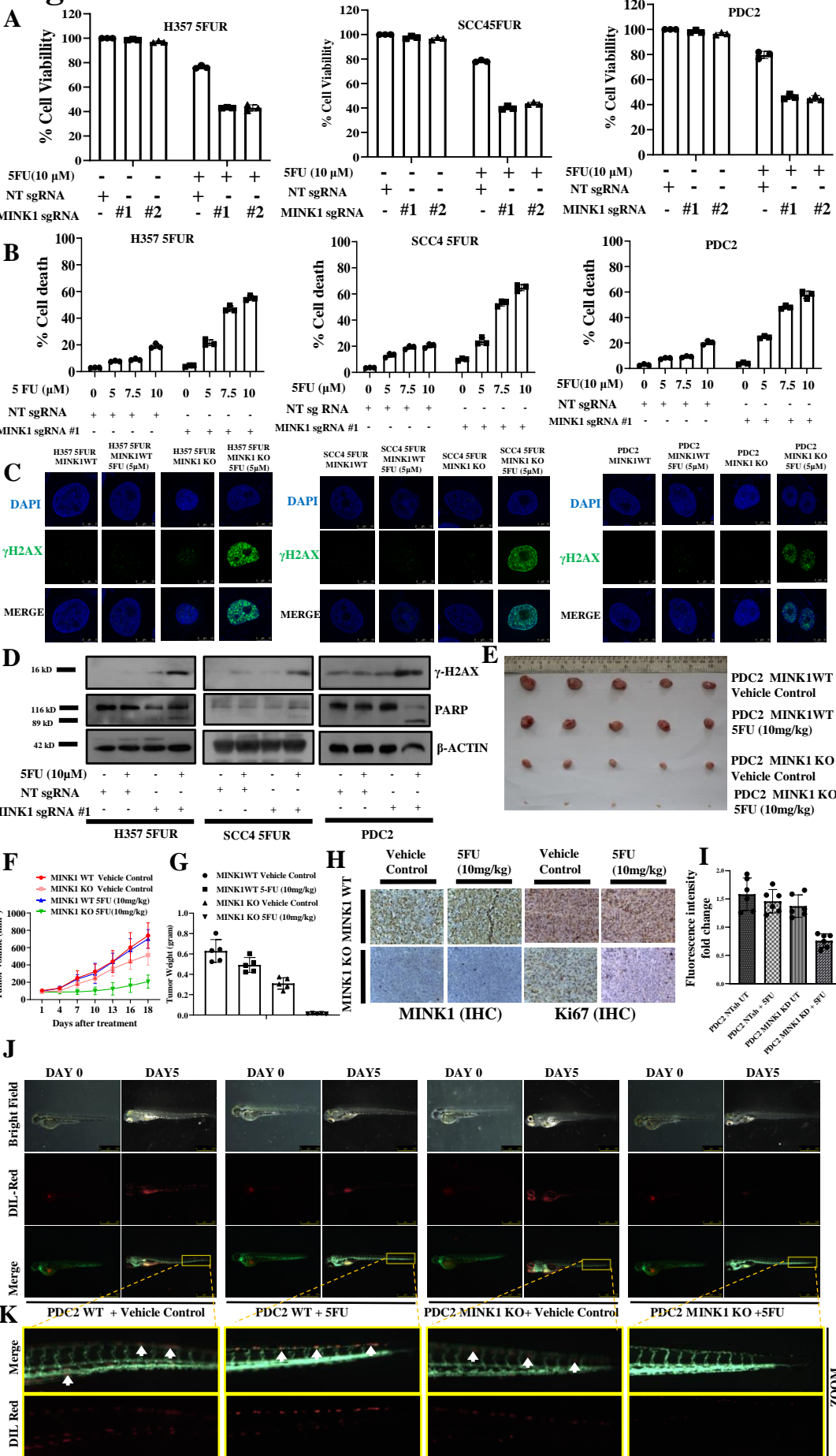


Figure 03

A

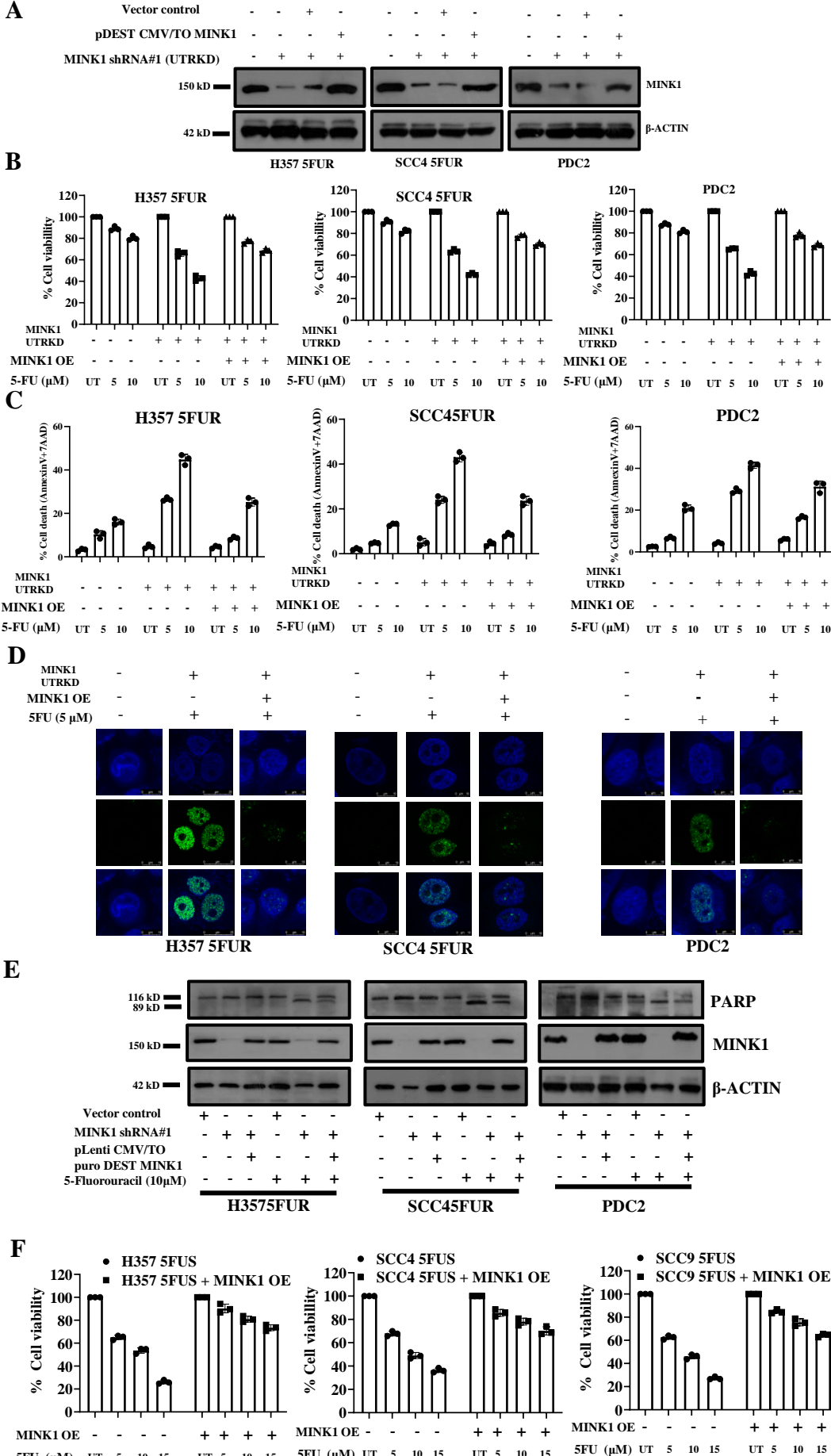


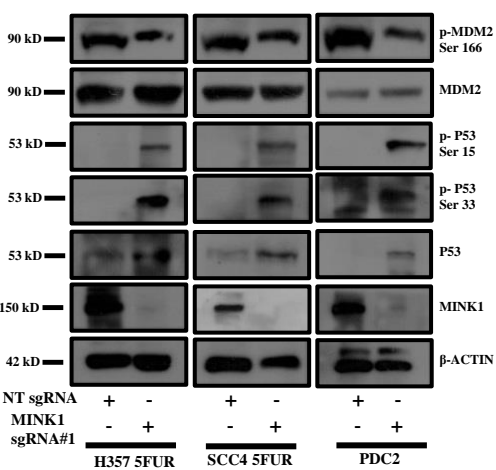
Figure 04

A

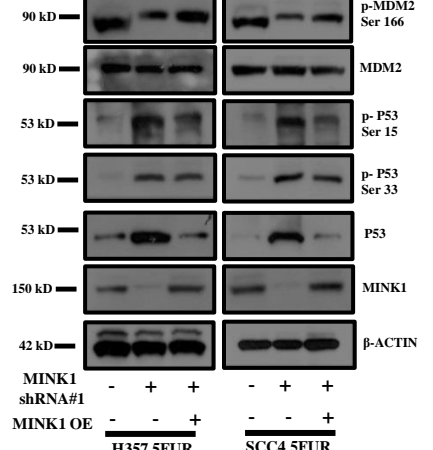
Phosphorylated proteins	Phosphorylation ratio of MINK1 KO/WT
c-Jun (Phospho-Ser13)	2.387529
ALK (Phospho-Tyr507)	2.187586
GSK3 beta (Phospho-Ser9)	2.172644
Gab2 (Phospho-Tyr543)	2.016942
AKT1 S11 (Phospho-Thr246)	2.008168
c-Jun (Phospho-Ser15)	1.920548
c-Jun (Phospho-Ser63)	1.897019
Catenin beta (Phospho-Tyr554)	1.799196
Keratin 6 (Phospho-Ser432)	1.751952
IL-13R/CD213c1 (Phospho-Tyr405)	1.641146
Dck-2 (Phospho-Tyr299)	1.604889
VEGFR2 (Phospho-Tyr1175)	1.600504
GSK3 alpha (Phospho-Ser21)	1.588892
Androgen Receptor (Phospho-Ser213)	1.566496
Tax (Phospho-Thr181)	1.566912
IGF2R (Phospho-Ser249)	1.565716
eIF-2A (Phospho-Ser51)	1.559497
COK5 (Phospho-Tyr15)	1.547983
14-3-3 zeta (Phospho-Ser58)	1.522109
4E-BP1 (Phospho-Thr55)	1.505419

Phosphorylated proteins	Phosphorylation ratio of MINK1 KO/WT
HDAC1 (Phospho-Ser421)	0.32937
AKT1 (Phospho-Tyr527)	0.351857
LYN (Phospho-Tyr527)	0.356728
Abp1 (Phospho-Tyr24)	0.403395
HSL (Phospho-Ser554)	0.492955
ATP1A1(NavK+NaV1.5) (Phospho-Ser23)	0.494441
EEF2 (Phospho-Thr56)	0.47177
TYRO (Phospho-Tyr1564)	0.506242
JAK2 (Phospho-Tyr1007)	0.532182
CIN8 (Phospho-Ser116)	0.538779
FL35 (Phospho-Tyr599)	0.558251
EGFR (Phospho-Thr899)	0.560672
Glut1 (Phospho-Ser449)	0.581223
AurB (Phospho-Thr232)	0.580028
AKT2 (Phospho-Ser442)	0.584925
Integrin beta-1 (Phospho-Thr788)	0.585157
DYN1 (Phospho-Ser74)	0.598312
MINK1 (Phospho-Ser166)	0.61482
IL-6RA/CD130 (Phospho-Ser205)	0.627742
Caspase 9 (Phospho-Tyr153)	0.630743

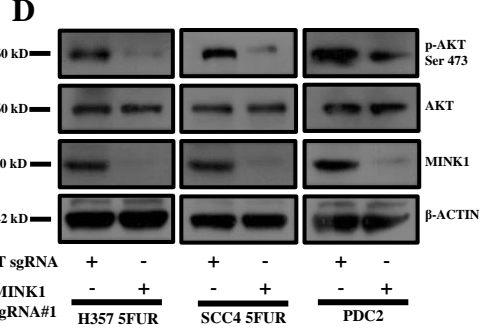
B



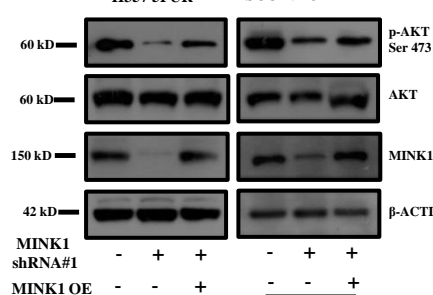
C



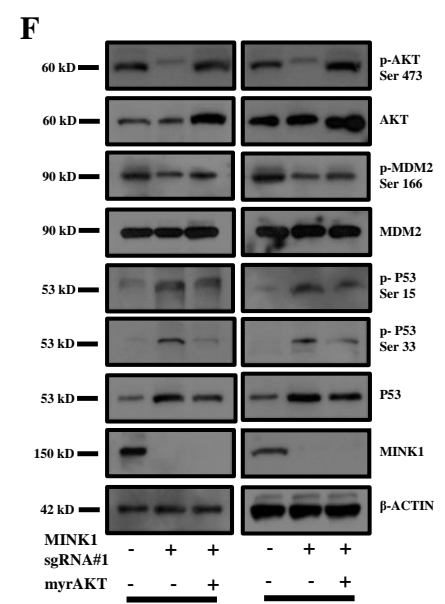
D



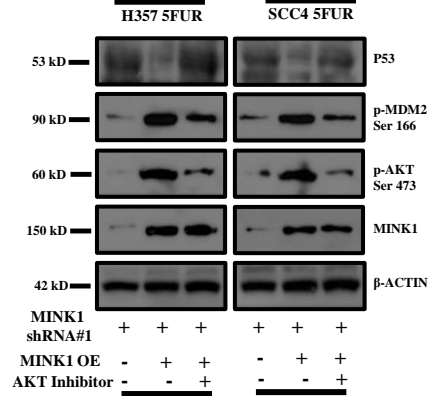
E



F



G



H

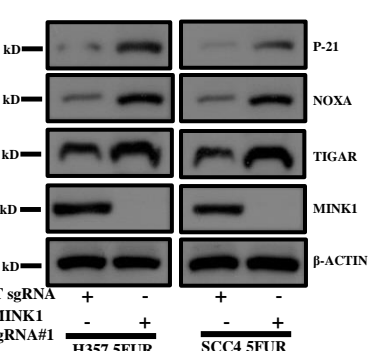


Figure 05

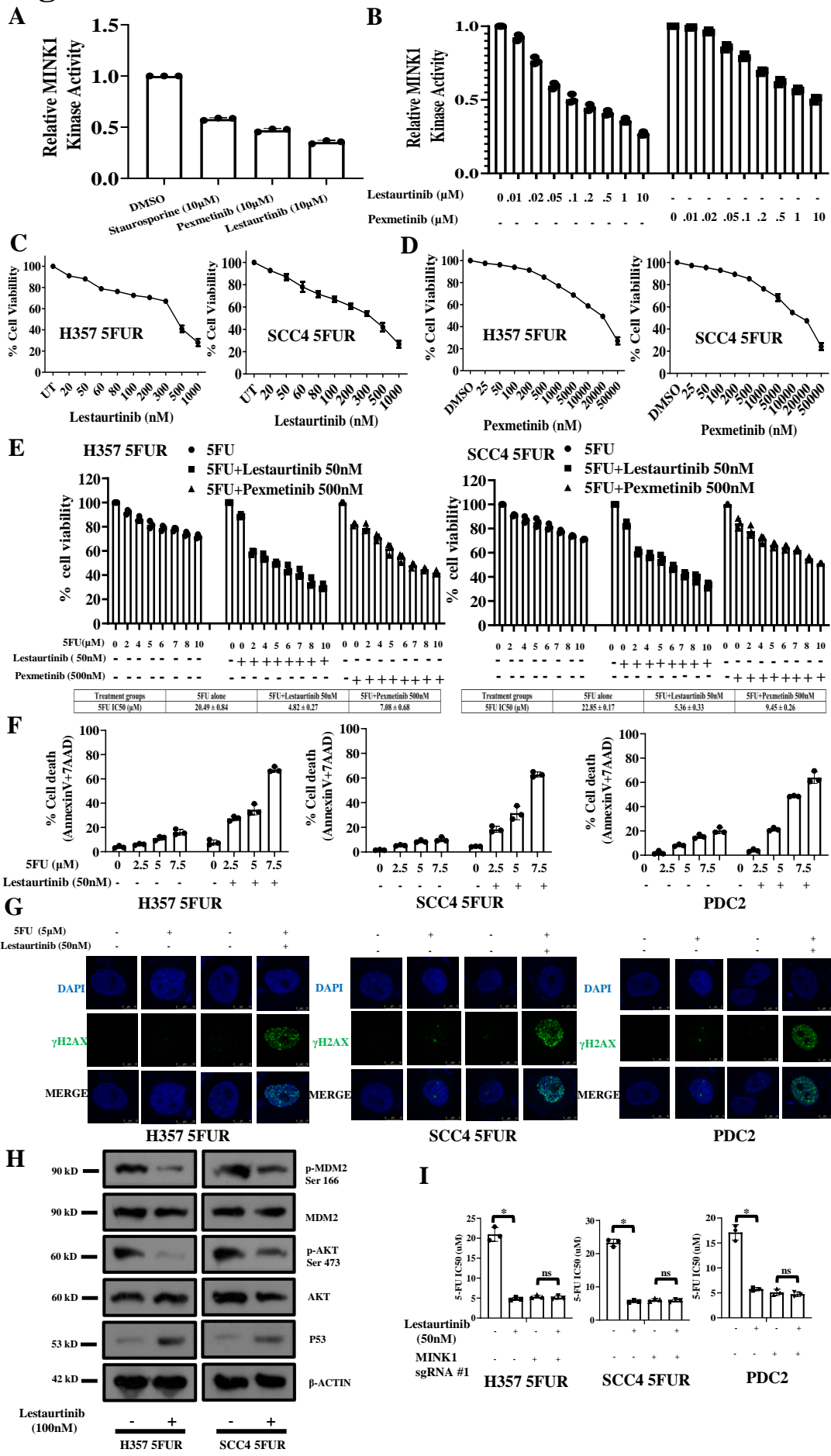


Figure 06

A



PDC2 Vehicle Control

PDC2
5FU(10mg/kg)

PDC2
Lestaurtinib (20mg/kg)

PDC2
5FU (10mg/kg) +
Lestaurtinib (20mg/kg)

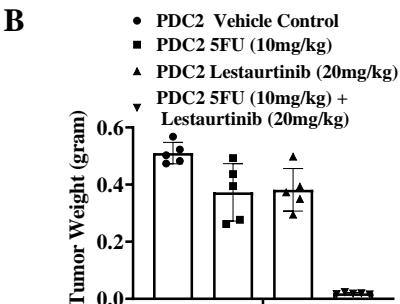


Figure 2: Tumor volume (mm³) vs Days after treatment for PDC2 Vehicle Control, PDC2 5FU (10mg/kg), PDC2 Lestaurtinib (20mg/kg), and PDC2 5FU(10mg/kg) + Lestaurtinib (20mg/kg) groups. The PDC2 5FU + Lestaurtinib group shows the lowest tumor volume, significantly lower than the other groups starting from day 10.

Days after treatment	PDC2 Vehicle Control	PDC2 5FU (10mg/kg)	PDC2 Lestaurtinib (20mg/kg)	PDC2 5FU(10mg/kg) + Lestaurtinib (20mg/kg)
1	~120	~120	~120	~120
4	~150	~150	~150	~150
7	~200	~180	~180	~180
10	~250	~220	~220	~200
13	~300	~280	~280	~250
16	~400	~350	~350	~300
18	~600	~550	~450	~200

D

PDC2 Vehicle Control	PDC2 5FU	PDC2 Lestaurtinib	PDC2 5FU + Lestaurtinib
			
			CD44
			
			Cleaved Caspase 3
			
			Ki67

E

5-Fluorouracil

Plasma membrane

Cytoplasm

Lestaurtinib

MINK1

Inactive

p-AKT Ser437

p-MDM2 Ser166

p53

Nucleus

p53

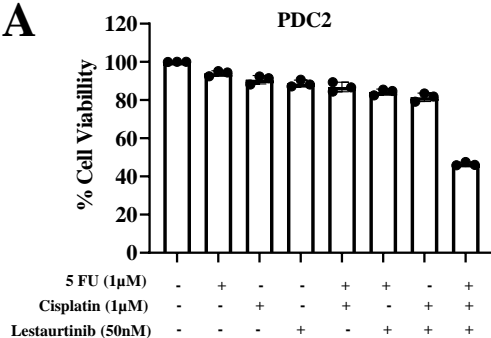
P21
NOXA
PUMA

CELL DEATH

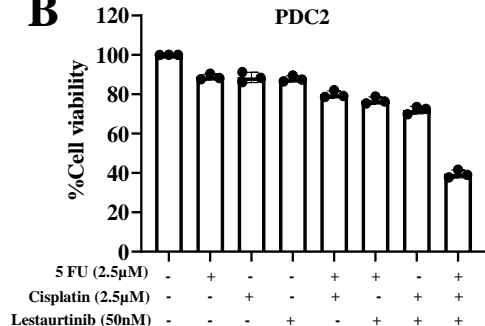
5FU Resistant OSCC cells

Figure 07

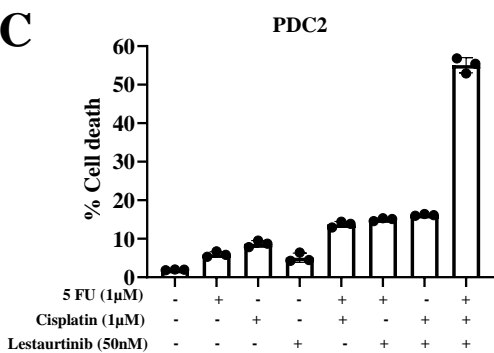
A



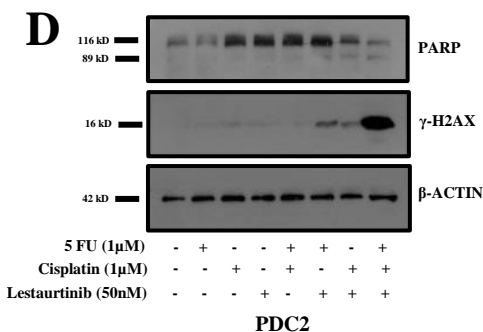
B



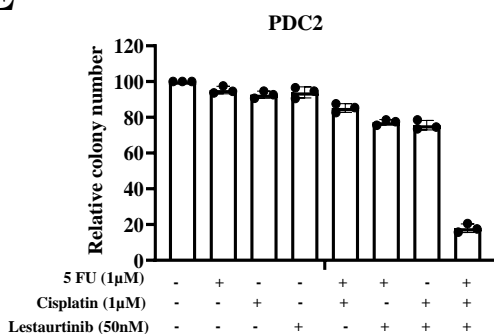
C



D



E



PDC2

